# Differentiation of primary and secondary marine organic aerosol with machine learning

Baihua Chen<sup>1</sup>, Lu Lei<sup>2</sup>, Emmanuel Chevassus<sup>2</sup>, Wei Xu<sup>1\*</sup>, Ling Zhen<sup>1</sup>, Haobin Zhong<sup>1</sup>, Lin Wang<sup>1</sup>, Chunshui Lin<sup>3</sup>, Ru-Jin Huang<sup>3</sup>, Darius Ceburnis<sup>2</sup>, Colin O'Dowd<sup>2</sup>, Jurgita Ovadnevaite<sup>2\*</sup>

- <sup>1</sup>State Key Laboratory of Advanced Environmental Technology, Institute of Urban Environment, Chinese Academy of Sciences, Xiamen, China.
  - <sup>2</sup>School of Physics, Centre for Climate & Air Pollution Studies, Ryan Institute, University of Galway, Galway, Ireland.
  - <sup>3</sup>State Key Laboratory of Loess and Quaternary Geology and Key Laboratory of Aerosol Chemistry and Physics, Institute of Earth Environment, Chinese Academy of Sciences, Xi'an, China.
- 10 Correspondence to: Wei Xu (wxu@iue.ac.cn) and Jurgita Ovadnevaite (jurgita.ovadnevaite@universityofgalway.ie)

Abstract. Marine primary organic aerosols (POA) are important components of the marine climate system, regulating solar radiation budget and cloud dynamics. Despite their importance, there is a lack of extensive long-term observations of POA properties, introducing great uncertainty in their parameterization in models. The lack of information originated from the complexity of POA chemical composition, very few long-term high-resolution measurements of clean marine air, and the difficulty in performing source apportionment techniques over a long-term period. In this study, we utilize a comprehensive high-resolution time-of-flight aerosol mass spectrometer dataset spanning a decade (2009-2018) and introduce a machine learning approach to distinguish between marine POA and marine secondary organic aerosol (SOA). Results indicate that marine POA concentrations peak during summer months and reach lowest levels in winter. On average, marine POA constitutes 51% (ranging from 21% to 76%) of the marine organic aerosol annually and up to 63% (48% to 75%) in summer. With the differentiated POA and SOA, we found diverse impacts of POA and SOA on aerosol hygroscopicity and mixing state. Increase in POA reduces the hygroscopicity and leads to external state of mixing, while the increase in SOA sustains the relatively high hygroscopicity and leads to internal mixing. This study provides observational dataset for marine POA and SOA and their diverse impacts on aerosol hygroscopicity, emphasizing a better appreciation of marine POA and SOA to improve the climate projections.

#### 5 1 Introduction

Marine aerosols constitute a large portion of the global aerosol budget and are pivotal in regulating the Earth's climate system (Fitzgerald, 1991; O'Dowd and Leeuw, 2007). It has been known for quite some time that marine aerosols contain a significant amount of organic matter (Blanchard, 1964). Cavalli et al. (2004) and O'Dowd et al. (2004) show the great contribution of organic matter in the Northeast Atlantic marine aerosol during periods of high biological activities. These marine organic aerosol originates from two sources: (1) bubble bursting that scavenges surface-active organic matter and other biogenic

materials (bacteria, viruses and detritus), producing primary organic aerosol (POA) (Barger and Garrett, 1970; Blanchard, 1964; Blanchard and Woodcock, 1957); (2) oxidation of marine volatile organic compounds (VOCs) such as dimethyl sulfide, aliphatic amines, isoprene and monoterpenes, which can form secondary organic aerosol (SOA) (Bates et al., 1992; Bonsang et al., 1988; Charlson et al., 1987; Facchini et al., 2008; Meskhidze and Nenes, 2006; Wohl et al., 2023; Zheng et al., 2020).

Marine POA is crucial for regulating cloud properties, acting as cloud condensation nuclei (CCN) or ice nuclei (IN). Ovadnevaite et al. (2011a) documented a marine POA plume with a peak POA concentration of up to 3.8 μg m<sup>-3</sup> in Northeast Atlantic, which is comparable to levels found in European continental air. Ovadnevaite et al. (2011b) further highlighted that marine POA has low hygroscopicity but high CCN potential. Additionally, sea spray tank experiments have demonstrated a significant correlation between seawater nanophytoplankton cell abundances and sea spray CCN number fluxes (Sellegri et al., 2021).

Incorporating marine POA into global models necessitates a comprehensive understanding of source strength and environmental response of POA. O'Dowd et al. (2008) proposed an integrated organic-inorganic sea spray source function that accounted for a size-dependent contribution of POA to total sea spray aerosol. Further parameterization efforts have considered factors such as chlorophyll-a concentration and wind speed (Gantt et al., 2011; Gantt et al., 2012; Rinaldi et al., 2013), which have been integrated into global chemical transport models. However, the influence of marine biota on the chemical composition and cloud activation properties of POA remains a contentious topic. O'Dowd et al. (2015) observed significant changes in the CCN activities of sea spray aerosol during a phytoplankton plume over Northeast Atlantic, whereas Quinn et al. (2014) and Bates et al. (2020) reported no substantial alterations in CCN activity over Northwest Atlantic.

In summary, the source intensity, chemical composition, mixing state, and cloud condensation activation potential of marine POA remain poorly understood (Gantt and Meskhidze, 2013) with large discrepancies between modelled and measured POA (Gantt et al., 2015). A major challenge in improving POA parameterization and modelling is the lack of long-term datasets, which are critical for both understanding the environmental drivers of POA emissions, and developing emission schemes for regional or global chemical transport models. The majority of the available data, such as that in Rinaldi et al. (2013), are derived from filter measurements that require extended sampling durations and result in low time resolution (days to weeks). Although filter-based methods can distinguish POA from SOA by using chemical molecular fingerprints (O'Dowd et al., 2004), they suffer from low temporal resolution, limiting their ability to capture dynamic changes in aerosol composition (minutes to hours).

The deployment of the Aerosol Mass Spectrometer (AMS) in both coastal and remote marine atmospheres has provided an opportunity to improve the POA parameterization and refine model predictions (Choi et al., 2017; Huang et al., 2018; Ovadnevaite et al., 2014; Saliba et al., 2020; Sanchez et al., 2020; Schmale et al., 2013; Willis et al., 2017). The AMS enables near-real-time measurements of aerosol chemical composition (DeCarlo et al., 2004, 2006), including organic aerosol (OA), non-sea salt sulfate (nss-SO<sub>4</sub>), ammonium (NH<sub>4</sub>), nitrate, methanesulphonic acid (Ovadnevaite et al., 2014) and sea salt

(Ovadnevaite et al., 2012). While POA and SOA can be differentiated using their mass spectra fingerprints through positive matrix factorization (PMF), this method faces challenges in high time resolution long-term data sets due to the required workforce and computational cost (Chevassus et al., 2024).

In this study, we developed a machine learning (ML) model to differentiate the contributions of marine POA and SOA from the measured total marine OA, using long-term marine aerosol measurements obtained by an AMS at the Mace Head Atmospheric Research Station. This model effectively identified and quantified contributions from the marine POA from SOA. The impacts of POA and SOA on aerosol hygroscopicity were then investigated.

#### 70 2 Methods

#### 2.1 Data and instrumentation

Aerosol measurements were conducted at the Mace Head Atmospheric Research Station (53°19′ N, 9°54′ W) on the west coast of Ireland from 2009 to 2018. The station, regularly exposed to clean marine air masses from the North Atlantic, has been a representative site for studying clean marine aerosols for several decades (O'Dowd et al., 2014).

We employed a High-Resolution Time-of-Flight AMS (DeCarlo et al., 2004) at Mace Head (Ovadnevaite et al., 2014) to measure the PM₁ (particulate matter with diameter smaller than 1 μm) chemical composition including organic aerosol (OA), non-sea-salt sulfate (nss-SO₄), sea salt, methanesulfonic acid (MSA) (Ovadnevaite et al., 2014), ammonium (NH₄), and nitrate (NO₃). Additionally, black carbon (BC) was measured using a Multi-Angle Absorption Photometer (MAAP) to trace anthropogenic emissions. Meteorological conditions were also recorded, including air temperature, pressure, precipitation, relative humidity, wind speed, and wind direction.

The humidified tandem differential mobility analyzer (HTDMA) (Swietlicki et al., 2000) was used to measure aerosol hygroscopic growth at a fixed relative humidity of 90% for aerosol with selected dried sizes of 35, 50, 75, 110, and 165 nm. The growth factors measured by HTDMA were inverted using a piecewise linear function (Gysel et al., 2009).

$$GF_{mean}^{a,b} = \frac{1}{nf^{a,b}} \int_{a}^{b} GF \ c(GF, D) dGF$$

5 The arithmetic mean GF ( $GF_{mean}$ ) was calculated as:

$$GF_{mean} = \int GF \ c(GF, D) dGF$$

To quantify the mixing state, the GF spread factor (SF), defined as the standard deviation of the GF-PDF divided by the  $GF_{mean}$ , was calculated as:

$$SF = \frac{\left(\int_0^\infty (GF - GF_{mean})^2 c(GF, D) dGF\right)^{1/2}}{GF_{mean}}$$

The GF was measured at 90% RH, however, the RH of the second DMA fluctuated slightly with the ambient temperature. The data between 88-92% RH were corrected using the κ-Köhler theory according to formula derived from Petters and Kreidenweis (2007):

$$\kappa = \frac{(GF^3 - 1)(1 - a_w)}{a_w} \rightarrow GF(a_w, \kappa) = \left(1 + \kappa \frac{a_w}{1 - a_w}\right)^{1/3}$$

where a<sub>w</sub> is the water activity, and obtained by Köhler theory:

$$a_w = \frac{RH}{\exp\left(\frac{4\sigma_s v_w}{RTD}\right)}$$

Where  $\sigma_s$  is the surface tension of the droplet,  $v_w$  is the partial molar volume of water, R is the universal gas constant, T is the temperature, and D is the diameter of the droplet. The surface tension is assumed to be 0.072 mN m<sup>-1</sup>.

Data from the AMS and MAAP were averaged to a 10-minute resolution, while the meteorological records were initially recorded hourly and later downscaled to 10-minute intervals using linear interpolation to enlarge the dataset's availability. Any gaps in the AMS or MAAP data that contain invalid measurements were removed. Hourly boundary layer heights were obtained from ERA5 (Hersbach et al., 2020) and downscaled to 10-minute resolution using linear interpolation.

# 2.2 Clean sector criteria and machine learning strategy

To differentiate between marine POA and SOA in Mace Head atmospheric research station (MHD), this study employs an ML model to predict the mass concentration of marine SOA. Subsequently, POA concentrations are obtained by subtracting SOA from the measured total OA. Marine SOA was chosen as the ML model predictor, because SOA is expected to be impacted by environmental factors and less is known about POA, emission strengthen and source regions. To ensure the high quality of the SOA production period, we implemented multiple screening criteria to minimize the influence of anthropogenic and marine primary signatures. First, we applied clean sector criteria, limiting BC concentration to less than 15 ng m<sup>-3</sup> and selecting wind

direction between 190 and 300 ° (O'Dowd et al., 2014), to exclude continental outflows and ship plumes. The clean sector criteria, which have been established and applied in various MHD research studies (O'Dowd et al., 2014; Ovadnevaite et al., 2014; Xu et al., 2022), were employed to isolate marine air masses from anthropogenic influences.

We then applied additional filtering processes to reduce the impact of POA production. We further refined the data by keeping instances with wind speed below 6 m/s and sea salt mass concentration under 0.03  $\mu$ g m<sup>-3</sup> to minimize the concentration of marine POA. Finally, we retained only those data points where nss-SO<sub>4</sub> was the dominant component (nss-SO<sub>4</sub>/OA > 4) to ensure a predominantly secondary source. We presumed that in these selected data, OA was predominantly SOA, with the contribution of POA represented by a minor and constant background concentration (POA<sub>bg</sub>).

Subsequently, we employed a support vector regression (SVR) (Awad et al., 2015) trained on these rigorously selected SOA production periods. SVR was chosen for its generalizability in handling small datasets and its resistance to overfitting (Ghimire et al., 2022; Juang and Hsieh, 2009). Unlike tree-based models like random forest (Breiman, 2001), SVR model can predict continuous values (Ma et al., 2003; Tang et al., 2024). The hyperparameters, including the penalty coefficient (C) and gamma (γ) of the Radial Basis Functions (RBF) kernel were tuned via grid research. The model targeted OA concentration, using nss-SO<sub>4</sub>, MSA, NH<sub>4</sub>, and meteorological parameters (temperature, relative humidity, boundary layer height, wind direction, and pressure) as predictors. We also included hours of the day to capture diurnal variations. Predictors not directly linked to secondary production, e.g., sea salt, NO<sub>3</sub>, and BC, are excluded to avoid over-fitting and ensure generalizability, even though including these might have enhanced the model performance in the training dataset. Wind speed was used to select the SOA production period, therefore, it was not suitable as a predictor. A summary of the variables employed as predictors is shown in Table 1. The SVR were trained using 'tidymodel 1.3.0' framework using R programming software (version 4.4.3).

Table 1. Predictors used for SOA ML model.

115

120

125

130

Predictors	Acronyms	Source	Rationale
Hour of the day	hour		to capture any diurnal pattern
nss-SO4	SO4	AMS measurement	Secondary aerosol marker
MSA	MSA	AMS measurement	Secondary aerosol marker
NH4	NH4	AMS measurement	Secondary aerosol marker
Temperature	temp	Meteorological records	Known to influence secondary processes
Rain	rain	Meteorological records	Related to wet removal
wind direction	wddir	Meteorological records	Related to sources
Boundary layer height	blh	ERA5 reanalysis	Related to concentration

The selected SOA production periods were split by the year 2015: data before 2015 were used to train the model. The training dataset covered a significant fraction of the variabilities of predictors, as illustrated in Fig. S1. The hyperparameters of the

SOA-SVR model were optimized using grid search and 5-fold cross validation. The data after 2015, which was unseen for the training process, was used to challenge the model's generalizability. Overall, there are 1700 hours of SOA production periods, and 477 hours (27.8%) after 2015.

135

140

A schematic diagram of the proposed methodology is shown in Fig. 1. Initially, the clean marine dataset was extracted by applying the clean sector criteria, followed by additional filtering processes to minimize the influence of POA. To assess the representativeness of the selected data as secondary sources, the Fuzzy C-Means (FCM) clustering method (Bezdek et al., 1984) was utilized. Subsequently, data were divided into training, validation, and test sets for ML, with SOA (including minor POA<sub>bg</sub>) as the predictive variable. To mitigate experimental uncertainties, cross-validation and Monte Carlo simulations were performed. The study further investigated the magnitude of the POA<sub>bg</sub> values. Finally, ML method was applied on the clean marine air masses data to predict marine SOA concentrations, enabling the differentiation of marine POA concentrations within the total marine OA.

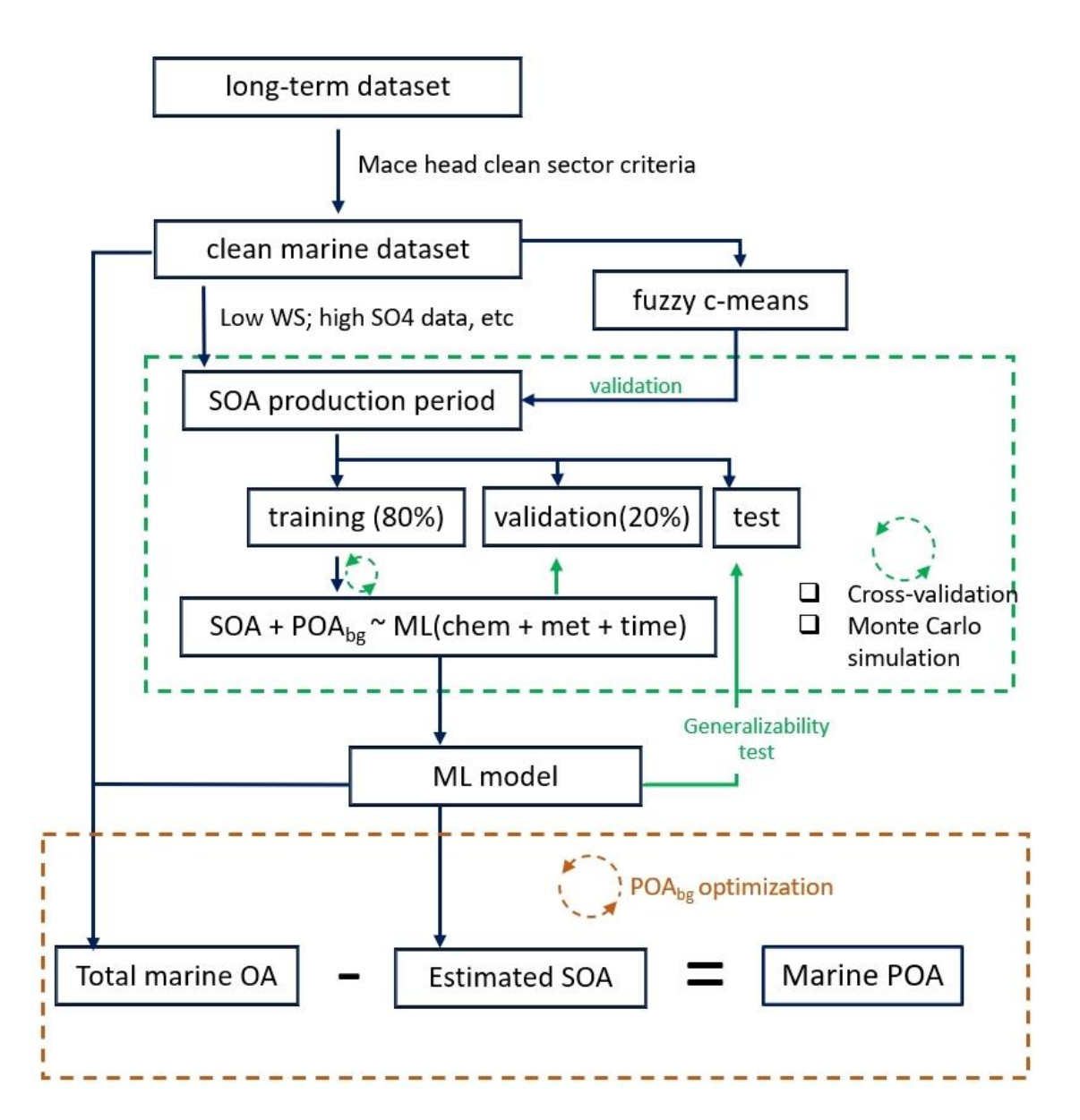


Figure 1. The proposed data processing and model construction workflow.  $POA_{bg}$  represents the assumed constant POA background concentration. ML (chem + met + time) represents the machine learning model that uses chemical composition, meteorological and time parameters as predictors.

## 2.3 Fuzzy-C Means clustering

FCM is a clustering algorithm that enables the grouping of data points into multiple clusters with varying degrees of membership. Unlike traditional hard clustering techniques, where each data point is assigned to a single cluster, FCM assigns membership levels to each data point, indicating the degree to which it belongs to each cluster. This soft clustering approach

is particularly useful when dealing with complex datasets where boundaries between clusters are not well-defined or overlap significantly. By optimizing an objective function that minimizes the weighted sum of squared errors, FCM iteratively updates the cluster centers and membership degrees, providing a flexible and robust means of uncovering underlying patterns and structures within data. In this study, the input variables for the FCM model included chemical components (SeaSalt, Org, NO3, SO4, NH4, MSA, and BC), as well as meteorological parameters — temperature (temp), relative humidity (rhum), wind speed (wdsp), and wind direction (wddir). We randomly selected 10,000 samples and retained only those with positive concentrations for all chemical components. The data were then log10-transformed and Z-score standardized. The FCM model was configured with 5 clusters, a fuzziness exponent of 1.2, and Euclidean distance as the distance metric.

#### 3 Results and Discussions

155

160

165

170

175

180

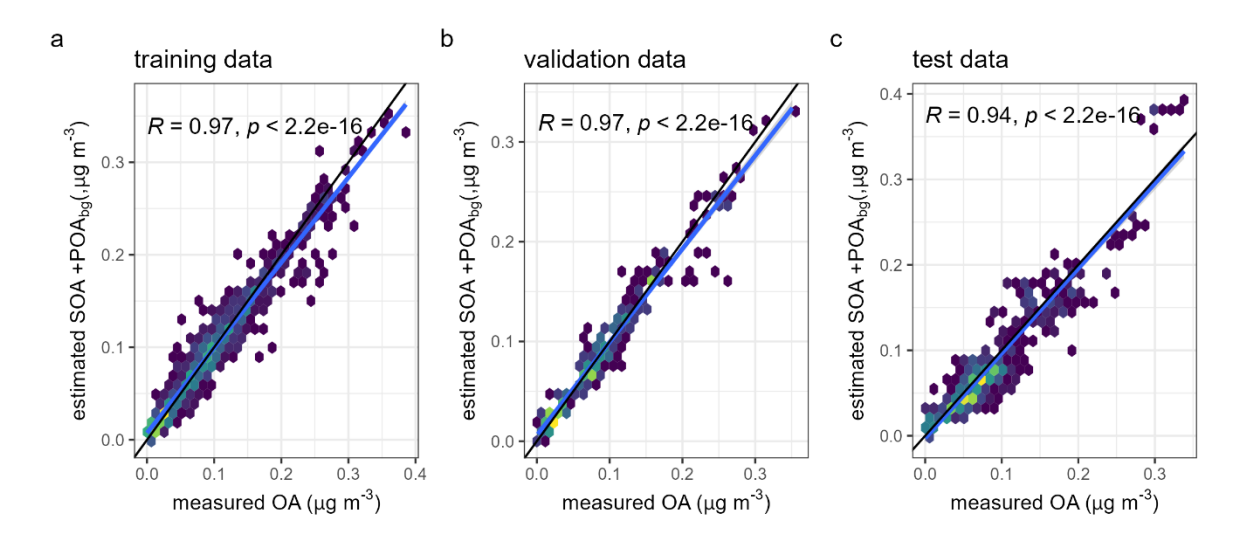
#### 3.1 Performance of ML model in SOA production period

We first examined the aerosol composition in the selected secondary marine aerosol dataset. In these SOA production periods, nss-SO<sub>4</sub> constituted  $68.9 \pm 8.7\%$  of the PM<sub>1</sub> mass, followed by OA at  $12.1 \pm 3.4\%$ , and MSA at  $6.8 \pm 4.0\%$ . The average concentration of sea salt and wind speed were  $0.015 \pm 0.009 \,\mu g$  m<sup>-3</sup> and  $4.6 \pm 1.2 \,m/s$ , respectively. The MSA to nss-SO<sub>4</sub> ratio was  $0.10 \pm 0.06$ , aligning with previous findings at the same site (Ovadnevaite et al., 2014). BC concentrations remained well below the 15 ng m<sup>-3</sup> threshold, averaging at  $6.0 \pm 3.7 \,n g$  m<sup>-3</sup>. Taken together, this chemical composition indicates the selected data mainly originated from secondary sources.

To ensure the representativeness of the selected training data as secondary sources, we applied FCM method on the clean marine dataset to identify the characteristics of chemical and meteorological parameters from typical sources. Compared to more conventionally used k-means clustering, FCM allows data instances to belong to multiple clusters with varying degrees of membership (or probability). The membership is used to determine how strongly each data instance belongs to each cluster. The FCM clustering, which is independent of the selection of SOA production periods, provides further validation and examination of the data selection for model training. We selected those with any cluster membership higher than 80% to show the clustering center of each cluster. As shown in Fig. S2a, the 2<sup>nd</sup> factor, which is featured by low sea-salt, low wind speed and high temperature, is most likely to be of the secondary origin. This factor also showed high MSA and nss-SO<sub>4</sub>, supporting the selection criteria for SOA production period. Indeed, the highest possibility of the selected training data is found to be the 2<sup>nd</sup> factor (Fig. S2b), reaffirming the SOA production characteristics.

Subsequently, we employed the SVR model, leveraging the clean marine dataset, to predict OA (SOA + POA<sub>bg</sub>) concentrations. Cross-validation yields Pearson's R of 0.97 for training and validation datasets, demonstrating the model's accuracy in predicting total OA (SOA + POA<sub>bg</sub>) concentration using the selected predictors. The slopes between estimated SOA +POA<sub>bg</sub> and measured OA were 0.97 for both the training and validation data, indicating robust pattern recognition across most concentration ranges. The model also exhibited great generalizability and performed consistently well on an unseen dataset

(Fig. 2c), with a Pearson's R value of 0.94 and a slope of 0.98 between observed OA and estimated SOA + POA<sub>bg</sub>, reaffirming the model's efficacy in modeling the complex dynamics of SOA.



185

190

195

Figure 2. Observed OA versus predicted ( $SOA + POA_{bg}$ ) for (a) training, (b) validation and (c) test datasets. Data density is illustrated using a color gradient with darker colour indicating lower data density. Black lines denote the 1:1 correspondence lines, blue lines represent regression lines.

Permutation importance analysis highlighted nss-SO<sub>4</sub> and MSA as the most influential variables, followed by NH<sub>4</sub> (Fig. 3a). Partial dependent plots (Fig. 3b) indicate a nonlinear relationship between SOA and increasing levels of nss-SO4 and MSA. While these plots do not imply a causal relationship, they highlight the complexity of the interactions and underscore the importance of employing a machine learning model to effectively capture such intricate patterns. Various meteorological parameters were also found to influence SOA concentration, especially relative humidity and precipitation, but to a lower extent. It should be noted that the nss-SO<sub>4</sub>, which albeit being marine secondary species, exhibit different formation dynamics and timescales with marine SOA, which might induce some extent of uncertainty. However, both marine SOA and nss-SO<sub>4</sub> might originate from marine biological activities. Furthermore, marine air masses arriving in MHD are expected to advected over Northeast Atlantic for several days. The use of nss-SO<sub>4</sub> can also be supported by the high correlation between nss-SO<sub>4</sub> and MSA, which exhibit different atmospheric formation dynamics.

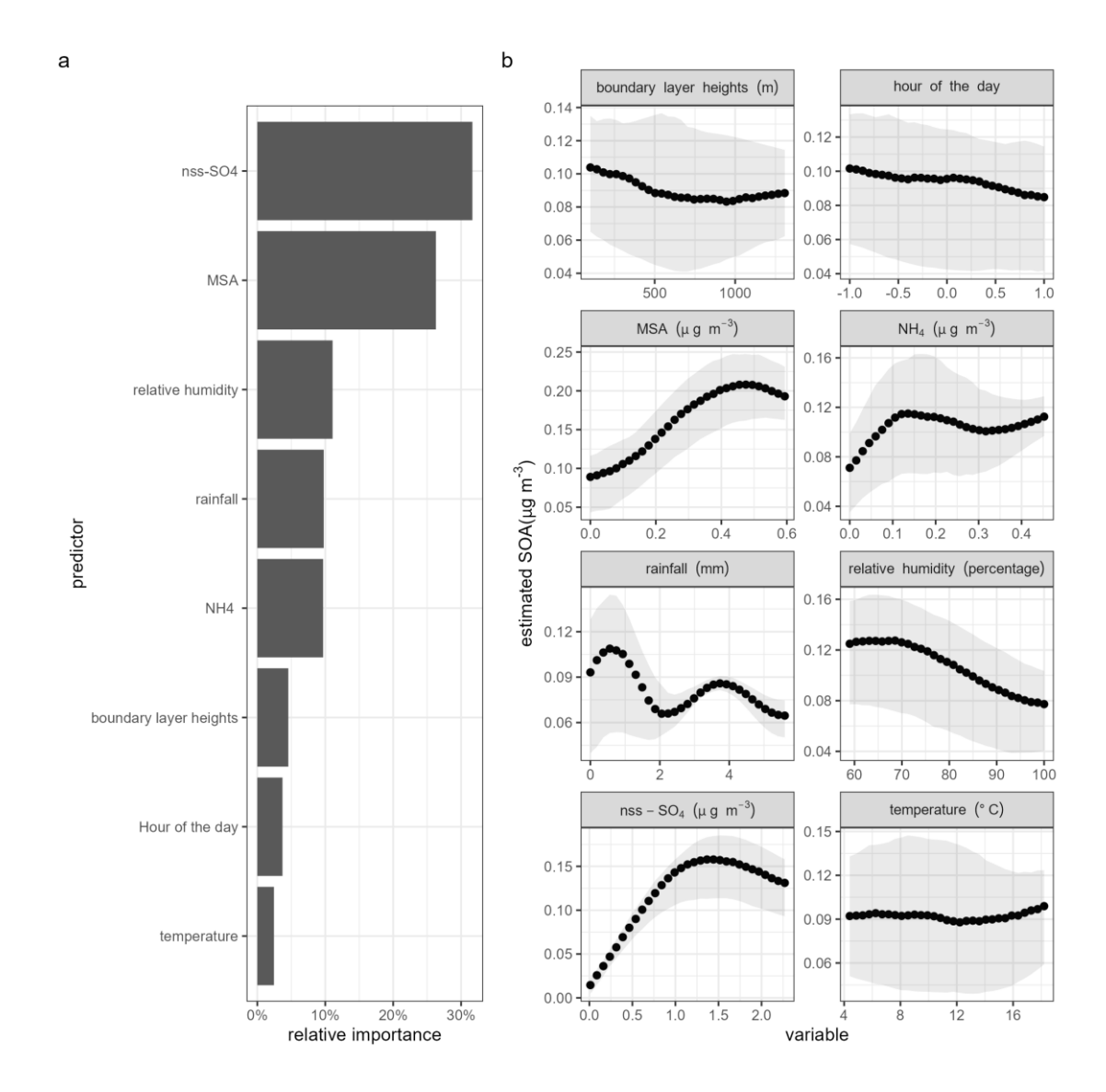


Figure 3. (a) the relative importance of different predictors. The hour and month were transformed with cosine functions. The month and hour were transformed to preserve continuity in the data. (b) The partial dependence of estimated SOA to different predictors. The lines represent median values and the shaded area represents 25<sup>th</sup> to 75<sup>th</sup> percentile; The 23:00pm and 01:00 am are numerically far apart while they are temporally close. Therefore, the hour of the day to periodic functions is simulated with cosine functions hour = cos(hour\*(2pi/12)).

205

In this study, one of the major assumptions of this approach is to assume that the OA in the selected secondary marine data for training the model is dominated by SOA. To evaluate the potential influence of POA contributions in those secondary marine data cases on entire clean marine dataset, we conducted a sensitivity analysis. We assumed that  $POA_{bg}$  constitutes 5% to 30%

of OA. As shown in Fig. S3, compared to the original assumption, the monthly averaged concentration of POA systematically increased throughout most of the year, except during winter, when alternative assumption predicted POA concentrations lower than 0, which is, of course, non-physical. Then, we applied the model on the entire clean marine dataset and tried different fixed POA<sub>bg</sub> values iteratively. As shown in Fig. S4, the POA<sub>bg</sub> of 0.01 µg m<sup>-3</sup> yields the least nonphysical predictions (either POA or SOA lower than 0). Therefore the POA<sub>bg</sub> of 0.01 µg m<sup>-3</sup> was used in the following calculation. Based on this strategy, SOA concentrations were predicted, enabling the estimation of POA concentrations. Furthermore, if POA production period is defined as periods with POA concentrations exceeding 0.1 µg m<sup>-3</sup> for more than 12 hours, there were more than 60 such POA production periods during the 10-year period (Fig. S5). Detecting these POA production periods allows for detailed characterization, potentially enhancing its parameterization.

Note that the measurement itself contains relatively large uncertainty, compared to summertime measurement. Indeed, we manually tuned the POA<sub>bg</sub> value to minimize the negative values. This is supported by previous studies that marine is a large organic pool (Quinn et al., 2014). Given the inherent uncertainties in aerosol measurements, as well-documented in previous study (Ovadnevaite et al., 2014), we further quantified the uncertainties associated with ML model using Monte Carlo simulations. To do this, we performed a robustness test by randomly validating the model 1000 times, each time excluding 20% of the data from the training set. The lower and upper limits of the estimated POA seasonality are shown in Fig. S6, which is similar to the original model. The Monte Carlo ensembles demonstrated negligible differences in the contribution of POA, indicating stable model performance across different scenarios. While it should be noted that the Monte Carlo bootstrapping is used to assess the random uncertainties, potential uncertainties associated with possible systematic uncertainties require further investigation.

To validate the ML-based POA concentrations, we further compared it with PMF-based POA concentrations from Chevassus et al. (2024). The PMF-based source apportionment was conducted for about one month. The Pearson's correlation coefficient between ML-based POA and PMF-based POA was about 0.91, indicating strong agreement between the two methods (Fig. 4). Compared to the conventional AMS-based OA source apportionment techniques, e.g., PMF, this ML approach requires significantly fewer computational resources and is less dependent on detailed knowledge of the mass spectra signatures of marine POA and SOA. For example, the model performed equally well even after removing MSA as a predictor (Fig. S7). Given that MSA can only be resolved by high-resolution AMS, this suggests that our approach could be extended to Aerosol Chemical Species Monitor (ACSM) data, which is more affordable and widely used but has lower mass resolution. This would enable broader applications of our method, offering a more comprehensive understanding of marine POA over global oceans. Finally, although secondary production of OA and nss-SO4 rely on similar meteorological conditions, it should be noted that many marine VOC species do not share the same sources and oxidization pathways as DMS and its derivatives. For example, some VOCs are produced by different organisms or abiotically from sea surface microlayer (Ciuraru et al., 2015; Mungall et al., 2017), which could introduce additional uncertainty in the SOA quantification based on high nss-SO4 periods, which adds to the uncertainty for POA attribution as well.

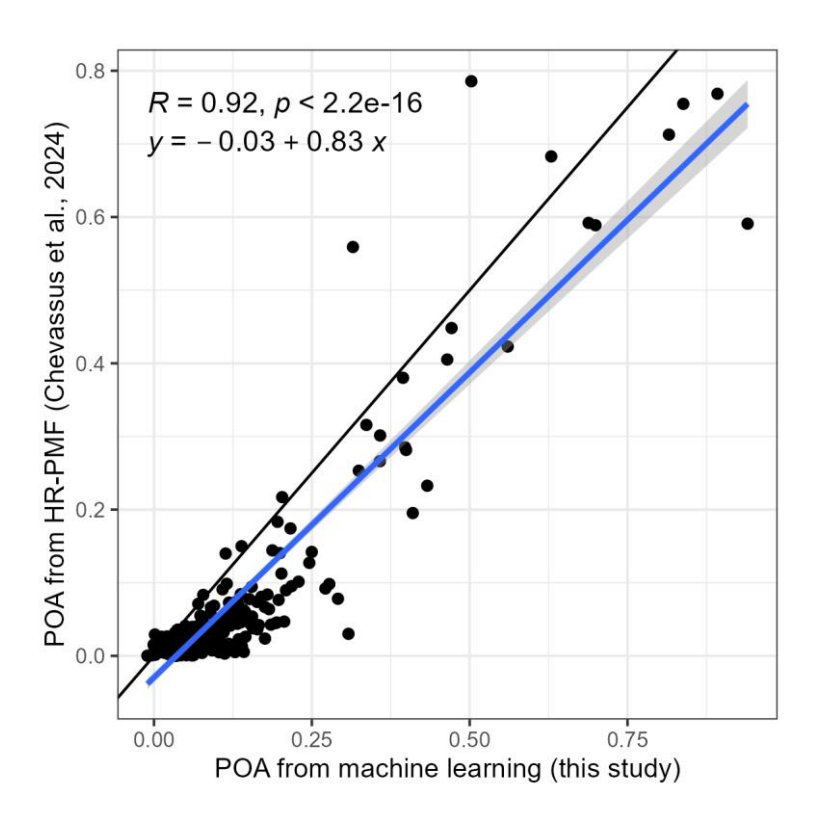


Figure 4. The comparison between machine learning-derived POA and HR-PMF POA. The HR-PMF POA data is taken from Chevassus et al. (2024). The blue line is regression line and grey area represents 95% confidence interval. The black line represents 1:1 line. Pearson's correlation coefficient and the equation of regression line are shown in the top left.

#### 3.2 Case study and long-term seasonality

245

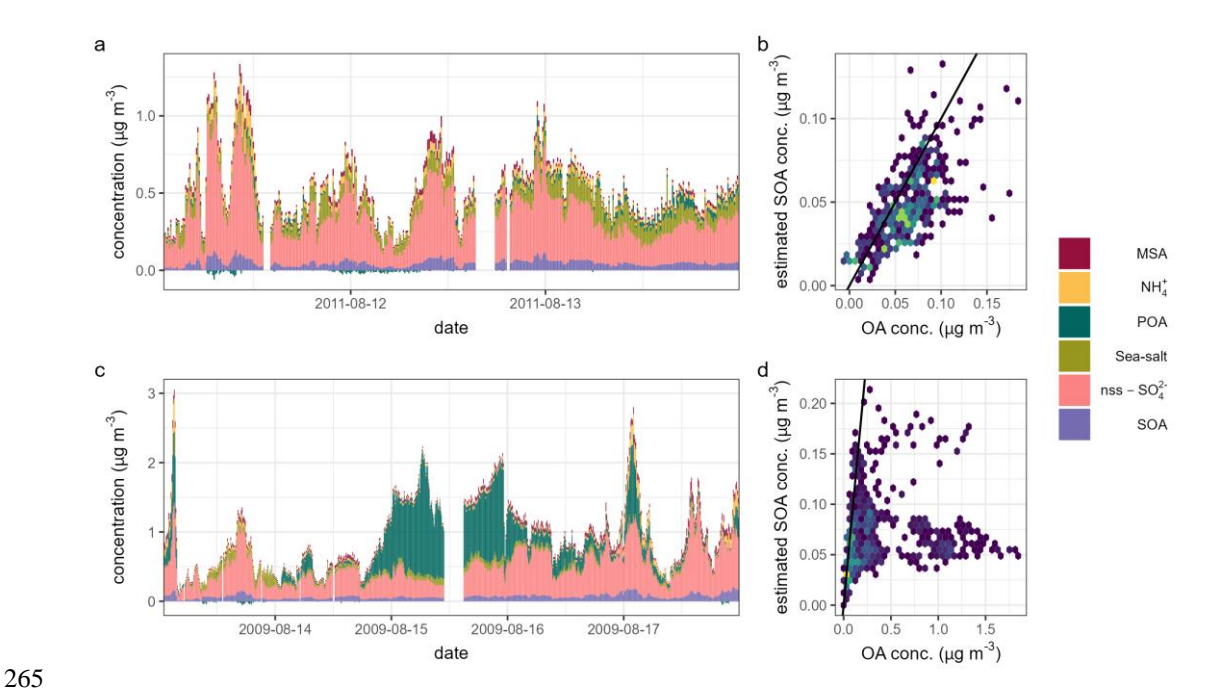
250

255

The evaluation of the model's performance has shown a clear relationship between SOA and the predictor variables in the chosen SOA production period. Assuming there is little and constant contribution from POA<sub>bg</sub>, the estimated SOA concentration should be similar to the measured OA. We then evaluated the model's performance in well-defined cases over finer time scales. During a typical SOA production period from  $11^{st}$  to  $14^{th}$  August 2011 (Fig. 4a), which was not included in the training dataset because of the slightly elevated sea salt above the threshold of  $0.03 \mu g m^{-3}$ , the measured OA closely followed the variation of nss-SO<sub>4</sub> and MSA, with Pearson's R values of over 0.80 and 0.84, respectively. These high correlations indicate a predominant secondary source of OA. The model's estimates of SOA concentrations were very close to the measured total OA (Fig. 4b), with an OA/SOA ratio of  $1.03 \pm 0.04$ . This further suggests that the ML model is able to predict the variability of SOA.

In contrast, during a well-documented marine POA plume, from 13<sup>rd</sup> to 18<sup>th</sup> August 2009 (Fig. 5c), the OA dominated the PM<sub>1</sub> concentration and showed little correlation with nss-SO<sub>4</sub> or MSA (Pearson's R of 0.05 and 0.08, respectively). Notably, the

estimated SOA deviates significantly from the observed OA (Fig. 5d). In this instance, the SOA estimated by the ML model accounted for only about 20% of the total OA during the plume, underscoring the significant contribution of marine POA. The different performance, presented in Fig. 5, is expected. In Fig. 5a, the model is mostly influenced by the nss-SO<sub>4</sub>, a marker for secondary species, leading to a great agreement between modelled SOA and observed OA. Conversely, Fig. 5d shows a significant discrepancy between modelled SOA and observed OA. The difference is largely attributed to the contribution of POA. This case was reported by Ovadnevaite et al. (2011a), in which the marine POA was identified using HR-ToF-AMS mass spectra, and the SOA during the period was not quantified.



260

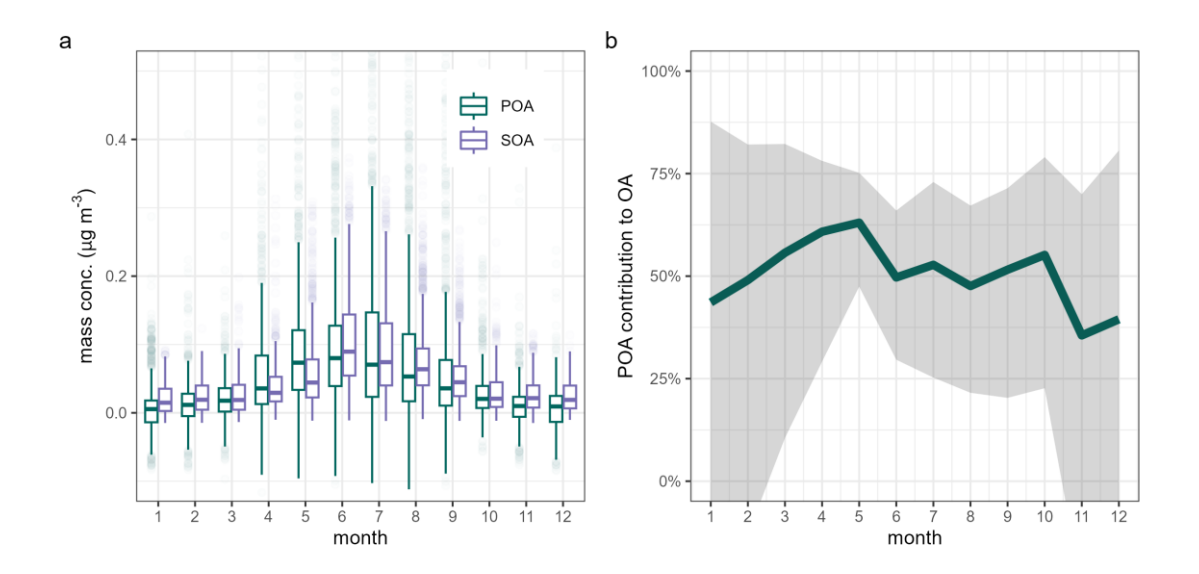
270

275

Figure 5. Case study of (a-b) SOA production period and (c-d) POA production period. (a,c) time series of PM<sub>1</sub> chemical species and (b,d) measured OA versus estimated SOA, the colour presents data density with darker colour indicating lower data density, the black lines represent 1:1 lines.

The cases of SOA and POA production periods indicate the model's capability to predict the SOA and POA levels. As illustrated in Fig. 6, both POA and SOA reached their peak in June and dropped to their lowest during the winter months. Typically, median concentrations of SOA were higher than those of POA across most months, except for May. However, POA concentrations spiked periodically, highlighted by outliers. The mean relative contribution of POA to total OA, detailed in Fig. 6b, shows the lowest contribution in winter and the largest from May to July, peaking at approximately 50% and slightly later in summer than SOA. The pattern corresponds with the enhanced marine activities in later spring and early summer of the North Atlantic, involving extensive phytoplankton proliferation and other marine organisms that release organic matter into the atmosphere through wave breaking and bubble bursting.

It is important to note that the total marine OA concentrations during winter at Mace Head are very low, introducing substantial uncertainty in OA separation during this season. The minimal POA concentration observed in winter suggests a distinct relationship between total OA, secondary species, and environmental factors. This relationship closely mirrors the dynamics observed in SOA. As shown in Fig. S8, the estimated SOA closely aligns with measured OA throughout the winter, pointing to low contribution from POA. Conversely, during the summer, numerous data points shown in Fig. S8 deviate to the right of the 1:1 lines, indicating a substantial contribution from POA.



280

285

290

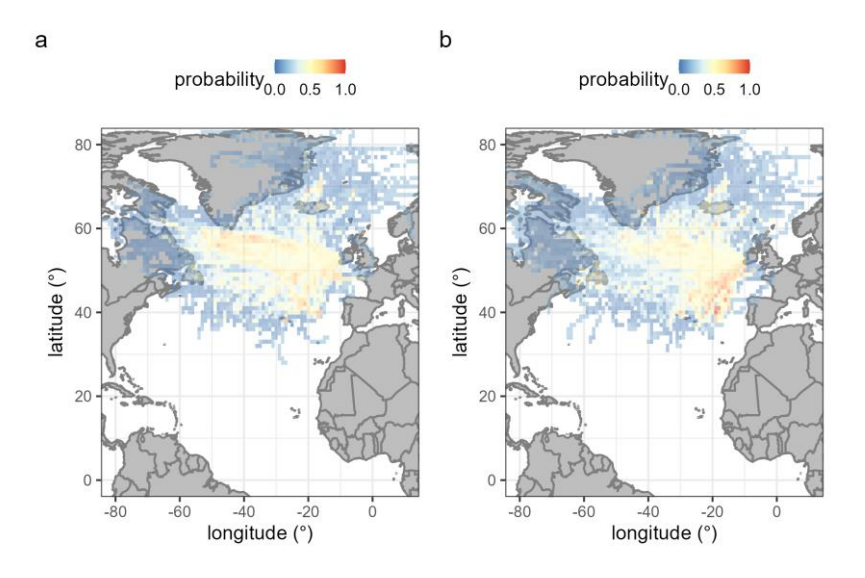
295

Figure 6. The seasonality of POA and SOA. (a) boxplot of mass concentration of POA (dark green) and SOA (purple), the horizontal lines represent median, the boxes represent 25<sup>th</sup> and 75<sup>th</sup> quantile, and the whiskers represent 1.5 inter-quarter ranges. Note that outliers are not fully shown to ease to visualization. (b)The contribution of POA to total OA, the line represents the monthly median, and the shaded area represents the 25<sup>th</sup> and 75<sup>th</sup> quantile.

The differentiation of POA from SOA is further substantiated by additional correlation analysis. As shown in Fig. S9, the correlation between OA and nss-SO<sub>4</sub> across the entire clean marine dataset is relatively low, at approximately 0.17, suggesting that nss-SO<sub>4</sub> explains less than 3% of the variability of marine OA. Upon decoupling the OA into POA and SOA, we observed distinct correlation patterns: the correlation between SOA and nss-SO<sub>4</sub> increased to 0.88, reflecting a strong linkage. Whereas for POA, it decreased to 0.08. This stark contrast underscores the different sources and atmospheric behaviors of marine POA and SOA. This different correlation analysis provides a clear delineation of how POA and SOA contribute to marine OA and emphasizes the capacity of advanced modeling techniques and long-term observations to unravel complex atmospheric processes.

The potential sources of POA and SOA were investigated using the Potential Source Contribution Function (PSCF) combined with air mass backward trajectories (Mansour et al., 2020). As shown in Fig. 7, POA likely originates from the Northeast

Atlantic polar marine regions (Fig. 7a), which are recognized as biologically active waters. In contrast, SOA sources are traced to tropical marine regions (Fig. 7b). The identified POA sources align with previous studies suggesting that regional marine biological activity is a key driver of POA production (O'Dowd et al., 2004; Sellegri et al., 2021). For SOA, enhanced photochemical reactions in lower-latitude waters likely promote the formation of secondary species. The distinct source regions of marine POA and SOA underscore the need for models to incorporate specific parameterisation schemes that account for these spatial and mechanistic differences.



300

310

315

Figure 7. The potential source contribution function analysis of marine POA (a) and SOA (b). Redish colour represents higher probability.

In contrast to prior studies that relied on filter-based measurements with limited temporal resolution, this study introduces a ML framework to systematically differentiate and quantify marine POA and SOA. While seasonal variations in POA/SOA have been reported previously, our decade-long dataset—the most extensive of its kind to date—provides unprecedented resolution to constrain and develop POA and SOA parameterization for climate models. Furthermore, the distinct source regions identified for POA (polar marine zones) and SOA (tropical waters) underscore their divergent formation mechanisms. Current model estimated of global emissions of POA span from 6.9 - 76 Tg year-1 for <1 µm emissions and global source of SOA were thought to be substantially smaller than marine POA. Our measurements found similar contribution of POA and SOA. While it has to be noted that some fraction of SOA were transformed via atmospheric aging from POA, which is difficult to quantify. Recent study found the photochemical reactions in the sea-air interface produce substantial VOC as the precursors of marine SOA (Brüggemann et al., 2018), the complex sources of SOA highlight the need for field observational data to challenge the models. The combined sensitivity to marine biological activities and photochemistry of marine OA was also supported by Sanchez et al. (2020), who found high correlation with downward shortwave flux and net primary production, while they did not separate POA and SOA.

## 3.3 Impact of marine organic aerosol to aerosol hygroscopicity and mixing state

The long-term marine POA and SOA time series now enable an assessment of their influence on aerosol hygroscopicity —a relationship previously uncertain. As shown in Fig. 8a, increasing POA concentrations from 0.1 to  $1~\mu g$  m<sup>-3</sup> reduces the hygroscopicity parameter ( $\kappa$ ) across all particle sizes, dropping values from  $\sim 0.5$  to below 0.25. This finding contrasts with earlier experimental work suggesting POA production has negligible effects on aerosol hygroscopicity and CCN activity (Quinn et al., 2014), but aligns with our prior case study highlighting the inherently low hygroscopicity of POA (Ovadnevaite et al., 2011b). Quinn et al. (2014) investigated the impact of marine POA on its cloud condensation nuclei using a sea sweep device, they found no significant difference of POA contribution at different oceanic regions with diverse ranges of chlorophyll-a, and they attributed the POA to the ocean carbon pool. However, based on our field measurements, it is unlikely that ocean carbon pool induces such large variations of the observed POA, underscoring the importance of oceanic biological activities.

As for the SOA, the increasing SOA concentrations from 0.1 to 0.3  $\mu$ g m<sup>-3</sup> only slightly reduce  $\kappa_{HTDMA}$  values (from 0.5 to 0.45) for particles between 50 and 165 nm, with no significant change observed for 35 nm particles. This muted response may arise from co-varying increases in secondary species such as nss-SO<sub>4</sub><sup>2-</sup> or MSA, which help maintain hygroscopicity at relatively high levels. This is consistent with our recent high-temporal online measurement, which shows a simultaneous increase in SOA and nss-SO<sub>4</sub><sup>2-</sup> during particle growth (Xu et al., 2024; Zheng et al., 2020). These results underscore the distinct roles of POA and SOA in modulating aerosol water uptake and cloud-forming potential, emphasizing the need to explicitly represent OA composition and sources in climate models.

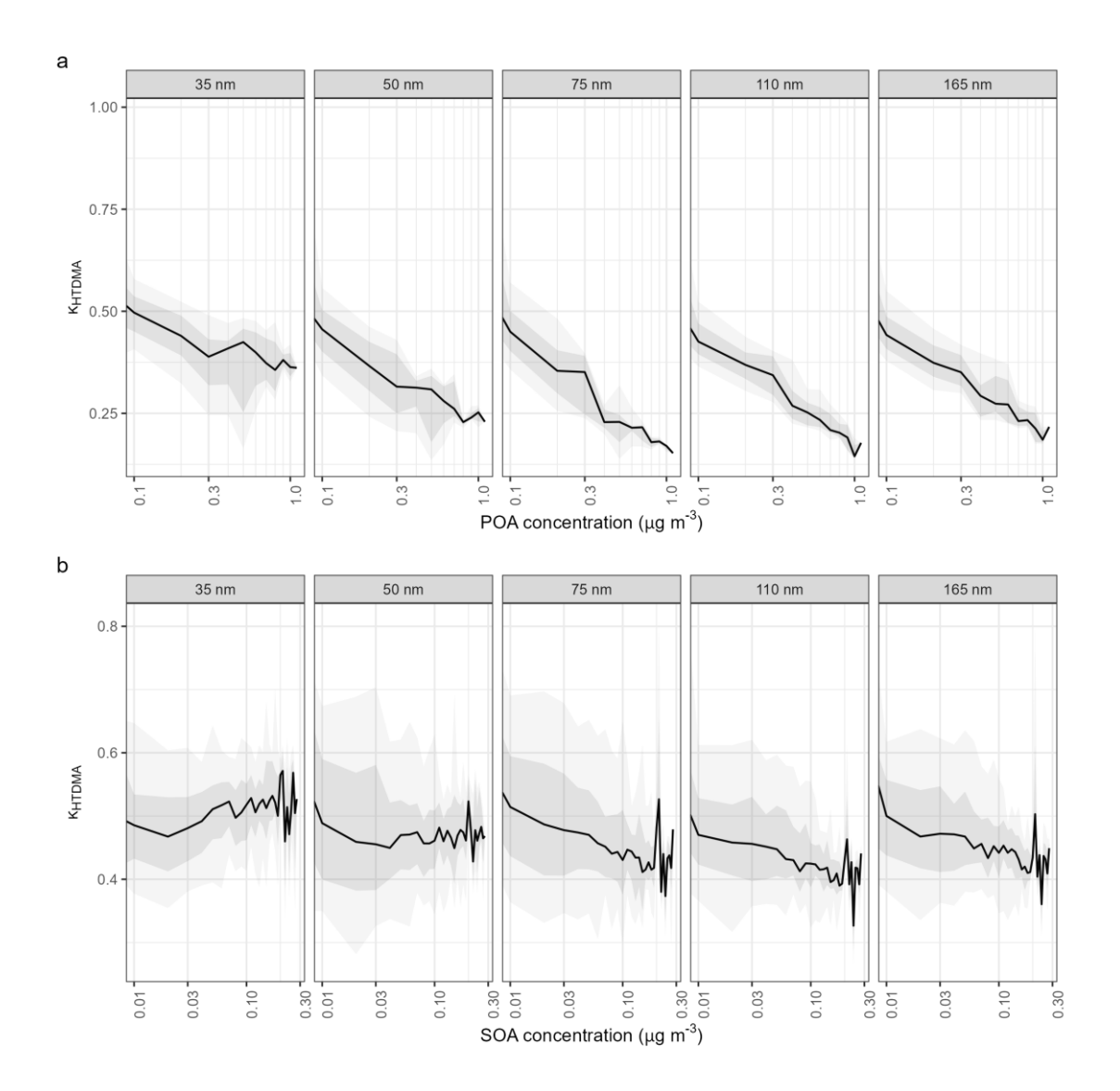


Figure 8. The impact of POA (a) and SOA (b) on aerosol hygroscopicity parameter (κ<sub>HTDMA</sub>) at different sizes. The analysis was limited to April to August to minimize the seasonal variations. The black lines represent medians, dark shaded areas represent 25<sup>th</sup> to 75<sup>th</sup> percentiles, darker shaded areas represent 10<sup>th</sup> to 90<sup>th</sup> percentiles.

340

345

The influence of POA and SOA on aerosol mixing state was further investigated using the spread factor, calculated from growth-factor probability density functions (Xu et al., 2020). A spread factor of 0 indicates a theoretically *internal* mixture, while higher values reflect increasing *external* mixing. Based on established thresholds (Swietlicki et al., 2008; Xu et al., 2019), a spread factor of ≤0.05 is classified as internal mixture, whereas values ≥0.2 signify external mixing. POA and SOA exhibit divergent impacts on aerosol mixing state. As shown in Fig. 9a, increasing the POA contribution from 0% to 100% elevates the spread factor, suggesting POA production promotes external mixing. Conversely, SOA accumulation drives the

system toward a more internally mixed state. This aligns with aerosol aging processes, where particles tend to homogenize over time. Accurately representing the hygroscopicity and mixing-state dynamics of POA and SOA is critical for assessing their climatic impacts, as these properties directly influence aerosol-cloud interactions and radiative forcing.

350

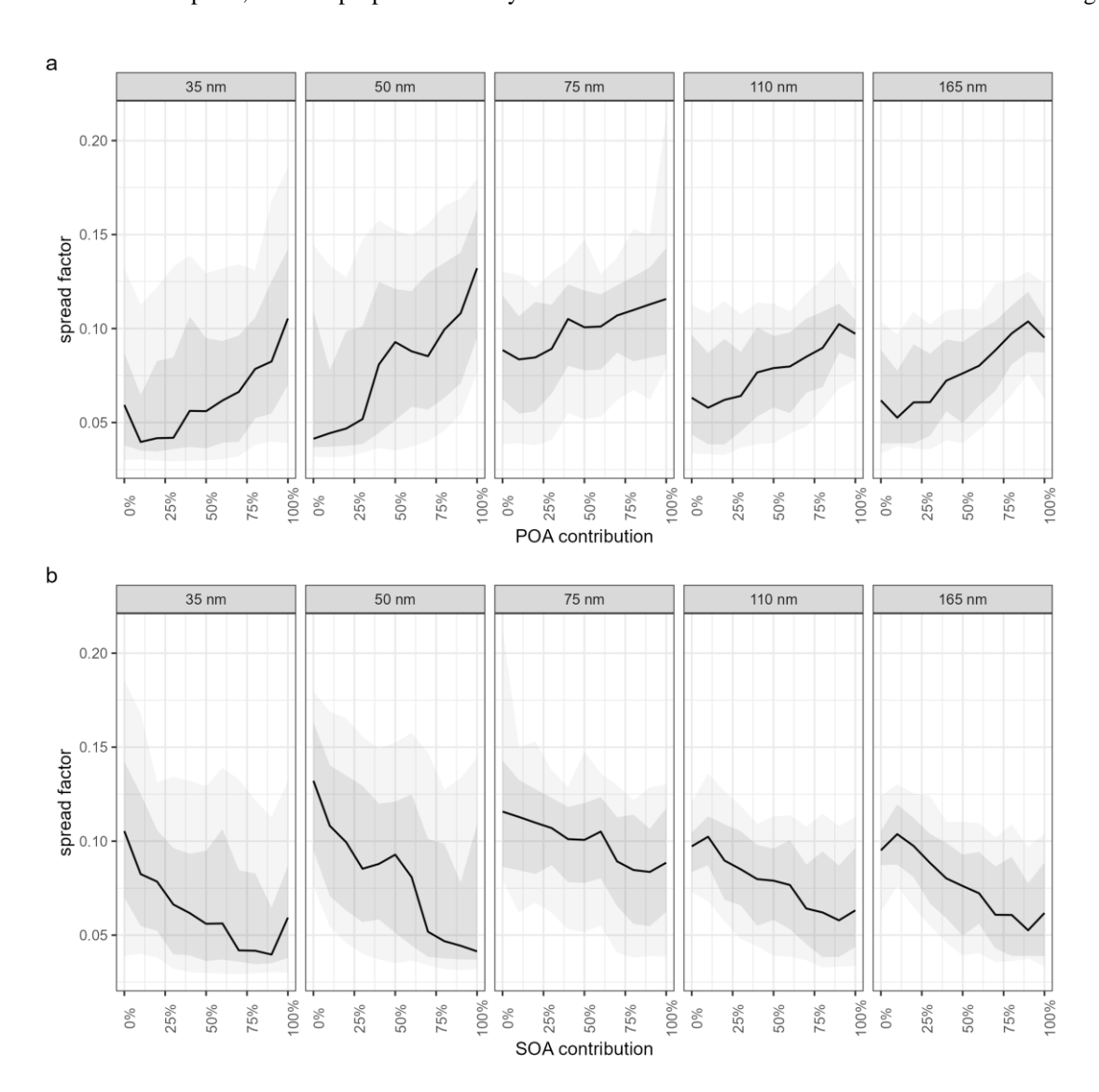


Figure 9. The impact of percentage contribution of POA (a) and SOA (b) to aerosol mixing state (spread factor) at different sizes. The analysis was limited to April to August to minimize the seasonal variations. The black lines represent medians, dark shaded areas represent 25<sup>th</sup> to 75<sup>th</sup> percentiles, darker shaded areas represent 10<sup>th</sup> to 90<sup>th</sup> percentiles.

## 355 4 Conclusion

360

365

375

380

Quantifying marine POA and SOA traditionally relies on PMF applied to aerosol mass spectra, which is challenging for long-term data. This study presents a data-driven ML framework to identify and quantify marine POA by leveraging temporal data patterns rather than chemical mass signatures. The ML model, trained on rigorously selected SOA-dominated periods, was applied to a multi-year aerosol dataset, enabling the identification of numerous POA production events. At Mace Head, marine POA constitutes ~50% of total marine organic aerosol (OA), increasing to 63% during late spring and early summer. Unlike PMF, this ML approach proves particularly effective for disentangling OA components in complex, long-term environments where high-resolution AMS data are unavailable.

Combined with aerosol hygroscopicity measurements, our analysis reveals distinct climatic impacts: marine POA significantly reduces aerosol hygroscopicity and promotes external mixing, whereas SOA exhibits weaker effects. These findings underscore the need to accurately quantify marine POA abundance and its influence on cloud-relevant properties. A key limitation lies in the selection of SOA-dominated periods for model training; future work should optimize ML performance for smaller or less curated datasets. Additionally, validating these marine POA results with global oceanic measurements is essential to refine POA parameterizations in climate and chemical transport models.

## **Supplement**

370 The supplement related to this article is available.

## Acknowledgement

This study is financial supported by National Key R&D Program of China (2023YFC3705503), the Guiding Project of Seizing the Commanding Heights of City Self-purifying Technology (No. IUE-CERAE-202403), Natural Science Foundation of China (No. 42307591), State Environmental Protection Key Laboratory of Formation and Prevention of Urban Air Pollution Complex, European Union's Horizon Europe Research and Innovation programme under HORIZON-CL5-2022-D1-02 (grant no. 101081430-PARIS), EPA-Ireland and the Department of Environment, Climate and Communications.

## Data availability

The AMS datasets used and/or analyzed during the current study are available on reasonable request from the corresponding author Jurgita Ovadnevaite (jurgita.ovadneviate@universityofgalway.ie). Aerosol hygroscopicity dataset is available via mendeley data (<a href="http://doi.org/10.17632/3dx6pnx869.1">http://doi.org/10.17632/3dx6pnx869.1</a>). ERA5 data is available from the CDS (<a href="https://cds.climate.copernicus.eu/#!/home">https://cds.climate.copernicus.eu/#!/home</a>).

# Code availability

The code is available upon request to the corresponding author (wxu@iue.ac.cn) and Jurgita Ovadnevaite (jurgita.ovadneviate@universityofgalway.ie).

#### 385 Author contribution

WX, LL and JO conceived the study, WX, BC, LZ, EC, CL, LW and HZ analyzed the data and constructed the models. JO and DC conducted the AMS and BC measurements. WX, RH and CO wrote the paper with the input from all the authors.

# **Declaration of Competing Interest**

The authors declare that they have no known competing financial interests or personal relationships that could have appeared to influence the work reported in this paper.

#### References

395

- Awad, M., Khanna, R., Awad, M., and Khanna, R.: Support vector regression, Efficient learning machines: Theories, concepts, and applications for engineers and system designers, 67–80, doi:https://dl.acm.org/doi/10.5555/2785649, 2015.
- Barger, W. and Garrett, W.: Surface active organic material in the marine atmosphere, Journal of Geophysical Research, 75, 4561–4566, doi:https://doi.org/10.1029/JC075i024p04561, 1970.
- Bates, T. S., Calhoun, J. A., and Quinn, P. K.: Variations in the methanesulfonate to sulfate molar ratio in submicrometer marine aerosol particles over the south pacific ocean, Journal of Geophysical Research: Atmospheres, 97, 9859–9865, doi: https://doi.org/10.1029/92JD00411, 1992.
- Bates, T. S., Quinn, P. K., Coffman, D. J., Johnson, J. E., Upchurch, L., Saliba, G., Lewis, S., Graff, J., Russell, L. M., and Behrenfeld, M. J.: Variability in Marine Plankton Ecosystems are not Observed in Freshly Emitted Sea Spray Aerosol over the North Atlantic Ocean, Geophysical Research Letters, doi:https://doi.org/10.1029/2019gl085938, 2020.
  - Bezdek, J. C., Ehrlich, R., and Full, W.: FCM: The fuzzy c-means clustering algorithm, Computers & Geosciences, 10, 191–203, https://doi.org/10.1016/0098-3004(84)90020-7, 1984.
  - Blanchard, D. C.: Sea-to-air transport of surface active material, Science, 146, 396–397, 1964.
- Blanchard, Dc. and Woodcock, A.: Bubble formation and modification in the sea and its meteorological significance, Tellus, 9, 145–158, doi: https://doi.org/10.3402/tellusa.v9i2.9094 ,1957.
  - Bonsang, B., Kanakidou, M., Lambert, G., and Monfray, P.: The marine source of c 2-c 6 aliphatic hydrocarbons, Journal of Atmospheric Chemistry, 6, 3–20, doi: https://doi.org/10.1007/BF00048328, 1988.
  - Breiman, L.: Random Forests, Machine Learning, 45, 5–32, doi:https://doi.org/10.1023/a:1010933404324, 2001.

- Brüggemann, M., Hayeck, N., and George, C.: Interfacial photochemistry at the ocean surface is a global source of organic vapors and aerosols, Nature Communications, 9, 2101, doi:https://doi.org/10.1038/s41467-018-04528-7, 2018.
  Cavalli, F., Facchini, M., Decesari, S., Mircea, M., Emblico, L., Fuzzi, S., Ceburnis, D., Yoon, Y., O'Dowd, C., Putaud, J.-P., et al.: Advancesin characterization of size-resolved organic matter in marine aerosolover the north atlantic, Journal of Geophysical Research: Atmospheres, 109, doi:https://doi.org/10.1029/2004JD005137, 2004.
- Charlson, R. J., Lovelock, J. E., Andreae, M. O., and Warren, S. G.: Oceanic phytoplankton, atmospheric sulphur, cloud albedo and climate, Nature, 326, 655–661, doi:https://doi.org/10.1038/326655a0, 1987.
  Chevassus, E., Fossum, K. N., Ceburnis, D., Lei, L., Lin, C., Xu, W., O'Dowd, C. D., and Ovadnevaite, J.: Marine organic aerosols at mace head: Effects from phytoplankton and source region variability, EGUsphere, 2024, 1–33, doi:https://doi.org/10.5194/egusphere-2024-2890, 2024.
- Choi, Y., Rhee, T. S., Collett, J. L., Park, T., Park, S.-M., Seo, B.-K., Park, G., Park, K., and Lee, T.: Aerosol concentrations and composition in the North Pacific marine boundary layer, Atmospheric Environment, 171, 165–172, doi: https://doi.org/10.1016/j.atmosenv.2017.09.047, 2017.
  Ciuraru, R., Fine, L., Pinxteren, M. van, D'Anna, B., Herrmann, H., and George, C.: Photosensitized production of
- doi:https://doi.org/10.1038/srep12741, 2015.
   DeCarlo, P. F., Slowik, J. G., Worsnop, D. R., Davidovits, P., and Jimenez, J. L.: Particle Morphology and Density Characterization by Combined Mobility and Aerodynamic Diameter Measurements. Part 1: Theory, Aerosol Science and Technology, 38, 1185–1205, doi:https://doi.org/10.1080/027868290903907, 2004.
   DeCarlo, P. F., Kimmel, J. R., Trimborn, A., Northway, M. J., Jayne, J. T., Aiken, A. C., Gonin, M., Fuhrer, K., Horvath, T.,

functionalized and unsaturated organic compounds at the air-sea interface, Scientific Reports, 5, 12741,

- Docherty, K. S., Worsnop, D. R., and Jimenez, J. L.: Field-Deployable, High-Resolution, Time-of-Flight Aerosol Mass Spectrometer, Analytical Chemistry, 78, 8281–8289, doi:https://doi.org/10.1021/ac061249n 2006.
   Facchini, M. C., Decesari, S., Rinaldi, M., Carbone, C., Finessi, E., Mircea, M., Fuzzi, S., Moretti, F., Tagliavini, E., Ceburnis, D., and O'Dowd, C. D.: Important Source of Marine Secondary Organic Aerosol from Biogenic Amines, Environmental Science & Technology, 42, 9116–9121, doi:https://doi.org/10.1021/es8018385, 2008.
- Fitzgerald, J. W.: Marine aerosols: A review, Atmospheric Environment. Part A. General Topics, 25, 533–545, 1991.

  Gantt, B. and Meskhidze, N.: The physical and chemical characteristics of marine primary organic aerosol: a review, Atmospheric Chemistry and Physics, 13, 3979–3996, doi:https://doi.org/10.5194/acp-13-3979-2013, 2013.

  Gantt, B., Meskhidze, N., Facchini, M. C., Rinaldi, M., Ceburnis, D., and O'Dowd, C.: Wind speed dependent size-resolved parameterization for the organic mass fraction of sea spray aerosol, Atmospheric Chemistry and Physics, 11, 8777–8790,
- doi:https://doi.org/10.5194/acp-11-8777-2011 2011.
  Gantt, B., Johnson, M. S., Meskhidze, N., Sciare, J., Ovadnevaite, J., Ceburnis, D., and O'Dowd, C. D.: Model evaluation of marine primary organic aerosol emission schemes, Atmospheric Chemistry and Physics, 12, 8553–8566, doi:https://doi.org/10.5194/acp-12-8553-2012, 2012.

- Ghimire, S., Bhandari, B., Casillas-Pérez, D., Deo, R. C., and Salcedo-Sanz, S.: Hybrid deep CNN-SVR algorithm for solar
- radiation prediction problems in Queensland, Australia, Engineering Applications of Artificial Intelligence, 112, 104860, https://doi.org/10.1016/j.engappai.2022.104860, 2022.
  - Gysel, M., McFiggans, G., and Coe, H.: Inversion of tandem differential mobility analyser (TDMA) measurements, Journal of Aerosol Science, 40, 134–151, doi:https://doi.org/10.1016/j.jaerosci.2008.07.013, 2009.
  - Hersbach, H., Bell, B., Berrisford, P., Hirahara, S., Horányi, A., Muñoz-Sabater, J., Nicolas, J., Peubey, C., Radu, R.,
- Schepers, D., Simmons, A., Soci, C., Abdalla, S., Abellan, X., Balsamo, G., Bechtold, P., Biavati, G., Bidlot, J., Bonavita, M., De Chiara, G., Dahlgren, P., Dee, D., Diamantakis, M., Dragani, R., Flemming, J., Forbes, R., Fuentes, M., Geer, A., Haimberger, L., Healy, S., Hogan, R. J., Hólm, E., Janisková, M., Keeley, S., Laloyaux, P., Lopez, P., Lupu, C., Radnoti, G., Rosnay, P. de, Rozum, I., Vamborg, F., Villaume, S., and Thépaut, J.-N.: The ERA5 global reanalysis, Quarterly Journal of the Royal Meteorological Society, 146, 1999–2049, doi:https://doi.org/https://doi.org/10.1002/qj.3803, 2020.
- Huang, S., Wu, Z., Poulain, L., Pinxteren, M. van, Merkel, M., Assmann, D., Herrmann, H., and Wiedensohler, A.: Source apportionment of the organic aerosol over the atlantic ocean from 53° n to 53° s: Significant contributions from marine emissions and long-range transport, Atmospheric Chemistry and Physics, 18, 18043–18062, doi: https://doi.org/10.5194/acp-18-18043-2018, 2018.
  - Juang, C.-F. and Hsieh, C.-D.: TS-fuzzy system-based support vector regression, Fuzzy Sets and Systems, 160, 2486–2504,
- 460 https://doi.org/10.1016/j.fss.2008.11.022, 2009.
  - Kreidenweis, S. M., Petters, M. D., and DeMott, P. J.: Single-parameter estimates of aerosol water content, Environmental Research Letters, 3, 035002,doi: https://doi.org/10.1088/1748-9326/3/3/035002, 2008.
  - Ma, J., Theiler, J., and Perkins, S.: Accurate On-line Support Vector Regression, Neural Computation, 15, 2683–2703, https://doi.org/10.1162/089976603322385117, 2003.
- Mansour, K., Decesari, S., Facchini, M. C., Belosi, F., Paglione, M., Sandrini, S., Bellacicco, M., Marullo, S., Santoleri, R., Ovadnevaite, J., Ceburnis, D., O'Dowd, C., Roberts, G., Sanchez, K., and Rinaldi, M.: Linking Marine Biological Activity to Aerosol Chemical Composition and Cloud-Relevant Properties Over the North Atlantic Ocean, Journal of Geophysical Research: Atmospheres, 125, doi:https://doi.org/10.1029/2019jd032246, 2020.
  - Meskhidze, N. and Nenes, A.: Phytoplankton and Cloudiness in the Southern Ocean, Science, 314, 1419–1423,
- 470 doi:https://doi.org/10.1126/science.1131779, 2006.
  - Mungall, E. L., Abbatt, J. P. D., Wentzell, J. J. B., Lee, A. K. Y., Thomas, J. L., Blais, M., Gosselin, M., Miller, L. A., Papakyriakou, T., Willis, M. D., and Liggio, J.: Microlayer source of oxygenated volatile organic compounds in the summertime marine Arctic boundary layer, Proceedings of the National Academy of Sciences, 114, 6203–6208, doi:https://doi.org/10.1073/pnas.1620571114, 2017.
- O'Dowd, C. and Leeuw, G. de: Marine aerosol production: a review of the current knowledge, Philosophical Transactions of the Royal Society A: Mathematical, Physical and Engineering Sciences, 365, 1753–1774, doi:https://doi.org/10.1098/rsta.2007.2043, 2007.

O'Dowd, C., Facchini, M. C., Cavalli, F., Ceburnis, D., Mircea, M., Decesari, S., Fuzzi, S., Yoon, Y. J., and Putaud, J.-P.: Biogenically driven organic contribution to marine aerosol, Nature, 431, 676–680, doi:https://doi.org/10.1038/nature02959,

480

2004.

- O'Dowd, C., Ceburnis, D., Ovadnevaite, J., Vaishya, A., Rinaldi, M., and Facchini, M. C.: Do anthropogenic, continental or coastal aerosol sources impact on a marine aerosol signature at Mace Head?, Atmospheric Chemistry and Physics, 14, 10687–10704, doi: https://doi.org/10.5194/acp-14-10687-2014, 2014.
- O'Dowd, C. D., Langmann, B., Varghese, S., Scannell, C., Ceburnis, D., and Facchini, M. C.: A combined organic-inorganic sea-spray source function, Geophysical Research Letters, 35, doi:https://doi.org/10.1029/2007gl030331, 2008.
  - O'Dowd, C. D., Ceburnis, D., Ovadnevaite, J., Bialek, J., Stengel, D. B., Zacharias, M., Nitschke, U., Connan, S., Rinaldi, M., Fuzzi, S., Decesari, S., Facchini, M. C., Marullo, S., Santoleri, R., Dell'Anno, A., Corinaldesi, C., Tangherlini, M., and Danovaro, R.: Connecting marine productivity to sea-spray via nanoscale biological processes: Phytoplankton Dance or Death Disco?, Scientific Reports, 5, 1, 11, doi:https://doi.org/10.1038/srep14883, 2015.
- Ovadnevaite, J., O'Dowd, C., Dall'Osto, M., Ceburnis, D., Worsnop, D. R., and Berresheim, H.: Detecting high contributions of primary organic matter to marine aerosol: A case study, Geophysical Research Letters, 38, 2011a.
   Ovadnevaite, J., Ceburnis, D., Martucci, G., Bialek, J., Monahan, C., Rinaldi, M., Facchini, M. C., Berresheim, H., Worsnop, D. R., and O'Dowd, C.: Primary marine organic aerosol: A dichotomy of low hygroscopicity and high CCN activity, Geophysical Research Letters, 38, L21806, doi:https://doi.org/10.1029/2011GL048869, 2011b.
- Ovadnevaite, J., Ceburnis, D., Canagaratna, M., Berresheim, H., Bialek, J., Martucci, G., Worsnop, D. R., and O'Dowd, C.: On the effect of wind speed on submicron sea salt mass concentrations and source fluxes, Journal of Geophysical Research: Atmospheres, 117, D16201, doi:https://doi.org/10.1029/2011JD017379, 2012.

  Ovadnevaite, J., Ceburnis, D., Leinert, S., Dall'Osto, M., Canagaratna, M., O'Doherty, S., Berresheim, H., and O'Dowd, C.:
  - Submicron NE Atlantic marine aerosol chemical composition and abundance: Seasonal trends and air mass categorization,
- 500 Journal of Geophysical Research: Atmospheres, 119, 11, 850–11, 863, doi:https://doi.org/10.1002/2013JD021330, 2014.
  - Quinn, P. K., Bates, T. S., Schulz, K. S., Coffman, D. J., Frossard, A. A., Russell, L. M., Keene, W. C., and Kieber, D. J.: Contribution of sea surface carbon pool to organic matter enrichment in sea spray aerosol, Nature Geoscience, 7, 228, 2014.
  - Rinaldi, M., Fuzzi, S., Decesari, S., Marullo, S., Santoleri, R., Provenzale, A., Hardenberg, J. von, Ceburnis, D., Vaishya, A., O'Dowd, C. D., and Facchini, M. C.: Is chlorophyll- a the best surrogate for organic matter enrichment in submicron primary
- 505 marine aerosol?, Journal of Geophysical Research: Atmospheres, 118, 4964–4973, doi:https://doi.org/10.1002/jgrd.50417, 2013.
  - Saliba, G., Chen, C., Lewis, S., Russell, L. M., Quinn, P. K., Bates, T. S., Bell, T. G., Lawler, M. J., Saltzman, E. S., Sanchez, K. J., Moore, R., Shook, M., Rivellini, L., Lee, A., Baetge, N., Carlson, C. A., and Behrenfeld, M. J.: Seasonal Differences and Variability of Concentrations, Chemical Composition, and Cloud Condensation Nuclei of Marine Aerosol
- $510 \quad over \ the \ North \ Atlantic, \ Journal \ of \ Geophysical \ Research: \ Atmospheres, \ doi: https://doi.org/10.1029/2020jd033145, \ 2020.$

- Sanchez, K. J., Zhang, B., Liu, H., Saliba, G., Chen, C.-L., Lewis, S. L., Russell, L. M., Shook, M. A., Crosbie, E. C., Ziemba, L. D., Brown, M. D., Shingler, T. J., Robinson, C. E., Wiggins, E. B., Thornhill, K. L., Winstead, E. L., Jordan, C., Quinn, P. K., Bates, T. S., Porter, J., Bell, T. G., Saltzman, E. S., Behrenfeld, M. J., and Moore, R. H.: Linking marine
- 515 Chemistry and Physics Discussions, doi:https://doi.org/10.5194/acp-2020-702, 2020.
  Schmale, J., Schneider, J., Nemitz, E., Tang, Y. S., Dragosits, U., Blackall, T. D., Trathan, P. N., Phillips, G. J., Sutton, M., and Braban, C. F.: Sub-antarctic marine aerosol: Dominant contributions from biogenic sources, Atmospheric Chemistry and Physics, 13, 8669–8694, doi:https://doi.org/10.5194/acp-13-8669-2013, 2013.

phytoplankton emissions, meteorological processes and downwind particle properties with FLEXPART, Atmospheric

- Sellegri, K., Nicosia, A., Freney, E., Uitz, J., Thyssen, M., Grégori, G., Engel, A., Zäncker, B., Haëntjens, N., Mas, S.,
- Picard, D., Saint-Macary, A., Peltola, M., Rose, C., Trueblood, J., Lefevre, D., D'Anna, B., Desboeufs, K., Meskhidze, N., Guieu, C., and Law, C. S.: Surface ocean microbiota determine cloud precursors, Scientific Reports, 11, 281, doi:https://doi.org/10.1038/s41598-020-78097-5, 2021.
  - Swietlicki, E., Zhou, J., Covert, D. S., Hameri, K., Busch, B., Vakeva, M., Dusek, U., Berg, O. H., Wiedensohler, A., Aalto, P. P., Makela, J., Martinsson, B. G., Papaspiropoulos, G., Mentes, B., Frank, G., and Stratmann, F.: Hygroscopic properties
- of aerosol particles in the north- eastern Atlantic during ACE-2, Tellus B: Chemical and Physical Meteorology, 52, 201–227, doi:https://doi.org/10.1034/j.1600-0889.2000.00036.x,2000.
  - Swietlicki, E., Hansson, H. C., Hämeri, K., Svenningsson, B., Maßling, A., McFiggans, G., McMurry, P. H., Petaja, T., Tunved, P., Gysel, M., Topping, D. O., Weingartner, E., Baltensperger, U., Rissler, J., Wiedensohler, A., and Kulmala, M.: Hygroscopic properties of submicrometer atmospheric aerosol particles measured with H-TDMA instruments in various
- environmentsa review, Tellus B: Chemical and Physical Meteorology, 60, 432–469, doi:https://doi.org/10.1111/j.1600-0889.2008.00350.x, 2008.
  - Willis, M. D., Köllner, F., Burkart, J., Bozem, H., Thomas, J. L., Schneider, J., Aliabadi, A. A., Hoor, P. M., Schulz, H., Herber, A. B., Leaitch, W. R., and Abbatt, J. P. D.: Evidence for marine biogenic influence on summertime Arctic aerosol, Geophysical Research Letters, 44, 6460–6470, doi:https://doi.org/10.1002/2017gl073359, 2017.
- Wohl, C., Li, Q., Cuevas, C. A., Fernandez, R. P., Yang, M., Saiz-Lopez, A., and Simó, R.: Marine biogenic emissions of benzene and toluene and their contribution to secondary organic aerosols over the polar oceans, Science Advances, 9, eadd9031, doi:https://doi.org/10.1126/sciadv.add9031, 2023.
  - Xu, W., Ovadnevaite, J., Fossum, K. N., Lin, C., Huang, R.-J., O'Dowd, C., and Ceburnis, D.: Aerosol hygroscopicity and its link to chemical composition in coastal atmosphere of mace head: Marine and continental air masses, Atmospheric
- 540 Chemistry and Physics, 2019, 1–25, doi:https://doi.org/10.5194/acp-2019-839, 2019.
  - Xu, W., Ovadnevaite, J., Fossum, K. N., Lin, C., Huang, R.-J., O'Dowd, C., and Ceburnis, D.: Aerosol hygroscopicity and its link to chemical composition in the coastal atmosphere of mace head: Marine and continental air masses, Atmospheric Chemistry and Physics, 20, 3777–3791, doi:https://doi.org/10.5194/acp-20-3777-2020, 2020.

- Xu, W., Ovadnevaite, J., Fossum, K. N., Lin, C., Huang, R.-J., Ceburnis, D., and O'Dowd, C.: Sea spray as an obscured
- $545 \quad source for marine cloud nuclei, Nature Geoscience, 15, \\ doi:https://doi.org/10.1038/s41561-022-00917-2, \\ 2022.$
- Xu, W., Ovadnevaite, J., Fossum, K. N., Huang, R.-J., Huang, D. D., Zhong, H., Gu, Y., Lin, C., Huang, C., O'Dowd, C., and Ceburnis, D.: Condensation of organic-inorganic vapours governs the production of ultrafine secondary marine cloud nuclei, Communications Earth & Environment, 5, 359, doi:https://doi.org/10.1038/s43247-024-01519-z, 2024.
  - Zheng, G., Kuang, C., Uin, J., Watson, T., and Wang, J.: Large contribution of organics to condensational growth and
- formation of cloud condensation nuclei (CCN) in remote marine boundary layer, doi: https://doi.org/10.5194/acp-20-12515-2020, 2020.
  - Ma, J., Theiler, J., and Perkins, S.: Accurate On-line Support Vector Regression, Neural Computation, 15, 2683–2703, https://doi.org/10.1162/089976603322385117, 2003.
  - Tang, D., Zhan, Y., and Yang, F.: A review of machine learning for modeling air quality: Overlooked but important issues,
- $555 \quad Atmospheric \ Research, \ 300, \ 107261, \ https://doi.org/10.1016/j. atmosres. 2024. 107261, \ 2024.$ 
  - Bezdek, J. C., Ehrlich, R., and Full, W.: FCM: The fuzzy c-means clustering algorithm, Computers & Geosciences, 10, 191–203, https://doi.org/10.1016/0098-3004(84)90020-7, 1984.
  - Breiman, L.: Random Forests, Machine Learning, 45, 5–32, https://doi.org/10.1023/a:1010933404324, 2001.
- Ghimire, S., Bhandari, B., Casillas-Pérez, D., Deo, R. C., and Salcedo-Sanz, S.: Hybrid deep CNN-SVR algorithm for solar
- radiation prediction problems in Queensland, Australia, Engineering Applications of Artificial Intelligence, 112, 104860, https://doi.org/10.1016/j.engappai.2022.104860, 2022.
  - Juang, C.-F. and Hsieh, C.-D.: TS-fuzzy system-based support vector regression, Fuzzy Sets and Systems, 160, 2486–2504, https://doi.org/10.1016/j.fss.2008.11.022, 2009.
- Ma, J., Theiler, J., and Perkins, S.: Accurate On-line Support Vector Regression, Neural Computation, 15, 2683–2703, https://doi.org/10.1162/089976603322385117, 2003.
  - Tang, D., Zhan, Y., and Yang, F.: A review of machine learning for modeling air quality: Overlooked but important issues, Atmospheric Research, 300, 107261, https://doi.org/10.1016/j.atmosres.2024.107261, 2024.